01 Feb 2016

Temperature Measurements during High Flux Ion Beam Irradiations

M. L. Crespillo

Joseph T. Graham
Missouri University of Science and Technology, grahamjose@mst.edu

Y. Zhang

W. J. Weber

Recommended Citation

M. L. Crespillo et al., "Temperature Measurements during High Flux Ion Beam Irradiations," *Review of Scientific Instruments*, vol. 87, no. 2, American Institute of Physics (AIP), Feb 2016.
The definitive version is available at https://doi.org/10.1063/1.4941720

REVIEW OF SCIENTIFIC INSTRUMENTS **87**, 024902 (2016)

Temperature measurements during high flux ion beam irradiations

M. L. Crespillo,[1,a)] J. T. Graham,[1,2,b)] Y. Zhang,[1,3] and W. J. Weber[1,3]
[1]*Department of Materials Science and Engineering, University of Tennessee, Knoxville, Tennessee 37996, USA*
[2]*Department of Mining and Nuclear Engineering, Missouri University of Science and Technology, Rolla, Missouri 65409, USA*
[3]*Materials Science and Technology Division, Oak Ridge National Laboratory, Oak Ridge, Tennessee 37831, USA*

(Received 8 October 2015; accepted 26 January 2016; published online 16 February 2016)

A systematic study of the ion beam heating effect was performed in a temperature range of −170 to 900 °C using a 10 MeV Au^{3+} ion beam and a Yttria stabilized Zirconia (YSZ) sample at a flux of 5.5×10^{12} cm^{-2} s^{-1}. Different geometric configurations of beam, sample, thermocouple positioning, and sample holder were compared to understand the heat/charge transport mechanisms responsible for the observed temperature increase. The beam heating exhibited a strong dependence on the background (initial) sample temperature with the largest temperature increases occurring at cryogenic temperatures and decreasing with increasing temperature. Comparison with numerical calculations suggests that the observed heating effect is, in reality, a predominantly electronic effect and the true temperature rise is small. A simple model was developed to explain this electronic effect in terms of an electrostatic potential that forms during ion irradiation. Such an artificial beam heating effect is potentially problematic in thermostated ion irradiation and ion beam analysis apparatus, as the operation of temperature feedback systems can be significantly distorted by this effect. © *2016 AIP Publishing LLC.* [http://dx.doi.org/10.1063/1.4941720]

I. INTRODUCTION

An important use of ion beams is in the modification and analysis of materials with uses in extreme environments, such as nuclear fission reactors, fusion reactors, and spacecraft.[1–3] In such environments, high temperatures are often present in addition to strong radiation fields. Some instances of ion beam analysis (IBA) make use of low temperatures, such as inducing phase changes, suppressing effects of atomic vibrations, enhancing optical and electronic properties, and for studying the energetics and kinetics of mobile defect species.[4–6] Therefore, temperature control plays an important role in the investigation of many physical phenomena in a wide variety of engineering materials.

Accurate measurement of sample temperatures is necessary in many experimental endeavors. Indeed, in systematic studies of ion beam material modification effects, annealing experiments, high and low temperature ion irradiations, etc., in which the changes in structure and properties strongly depend on the temperature of the material, the temperature is one of the most important experimental variables. For example, Schultz *et al.* reported large changes in the residual disorder in self-irradiated Si within the temperature range of 270-320 K.[7]

In vacuum systems, there are a limited number of standard techniques for measuring sample surface temperatures. The three principal techniques are the following: with thermocouples (TCs), pyrometry and with thermosensitive paints. Thermocouples are accurate provided they are well calibrated, they are rapid and provide near instantaneous temperature readout, and they are readily incorporated into a variety of ion beam apparatus. Thermocouples, however, act, to some degree, as heat sinks (or sources) and they are also susceptible to electronic interference. Pyrometers and infrared cameras have an advantage in that they make non-contact temperature measurements. Therefore, they do not perturb the sample temperature. However, their spatial resolution is limited by their optics. Furthermore, interpretation of pyrometer readings can be difficult. It depends on the accuracy of the temperature dependent emissivity of the material. Signals from hot materials near the measured sample can also interfere with the measured black body spectrum. This problem can also be compounded by the optical transparency of some bandgap materials. In ion beam experiments, ion beam induced luminescence (IBIL) can also produce non-black body light in the near infrared region, again interfering with the sample signal.

Thermosensitive paints represent a technique that relies on phase transitions occurring at discrete temperatures. Such phase transitions indicate when a specific temperature has been exceeded. These commercial paints are highly accurate in the sense that the temperature measured is absolute, albeit discrete (it does not rely on a calibration). Therefore, using thermosensitive paints complements other techniques that measure over a continuous temperature range. A disadvantage of these paints is that a portion of the sample surface must be sacrificed.

It is long known that ion beam heating can lead to temperature increases of hundreds of degrees in commercial ion implanters.[8] Pyrometry measurements of beam heating using 5 in. Si wafers in an ion implanter in the power density range of 0.1-200 W cm^{-2} showed heating up to the Si melting point.[9] Such beam heating occurs over large two-dimensional surfaces while the heat conduction is constrained primarily along one-dimension through the wafer thickness.

a)Electronic mail: mcrespil@utk.edu
b)Electronic mail: grahamjose@mst.edu

In the preparation of thin transmission electron microscopy (TEM) samples, significant heating can also take place. In one study, during ion thinning of Au/Si TEM specimens, the sample temperature was found to reach 370 °C.[10] In a focused ion beam (FIB), the areal power density can be orders of magnitude greater than for a parallel ion beam. Ishitani and Kaga calculated that, for a 30 keV Ga^+ beam with a power density of 7.6×10^4 W cm^{-2}, the temperature increases in Si, GaAs, and SiO_2 are 2.3, 8 and 427 °C, respectively.[11] Kempf *et al.* used laser interferometry to measure the beam heating of a 12 keV O_2^+ beam in a Au thin film.[12] The maximum temperature increase was 10 °C at power density of 75 W cm^{-2}. Beam power density, the geometry of the irradiation, and material properties are clearly important factors in deciding the change in temperature due to ion beam heating.

The experiments presented in this paper attempt to quantify the ion beam heating effect during ion irradiation with high fluxes and heavy ions at several different background temperatures with the aim of evaluating how critical an effect it can be. More importantly, this manuscript highlights an overlooked pitfall of *in-situ* temperature measurements in ion irradiation and ion beam analysis in that thermocouple measurements of the temperature can be completely unreliable under certain sample, beam, and temperature conditions.

II. EXPERIMENTAL

Beam heating effects were investigated through a series of high and low temperature experiments employing a beam of 10 MeV Au^{3+} ions at a flux of 5.5×10^{12} cm^{-2} s^{-1} at the Ion Beam Materials Laboratory at the University of Tennessee, Knoxville.[13] The choice of ion species and energy was based on the need for a high beam power. The greater the power deposited into the sample area, the better the chances for observing a beam heating effect. The areal power density corresponding to this beam is 8.8 W cm^{-2}. In the measurements, a $5 \times 5 \times 0.5$ mm sample of 8% Yttria stabilized Zirconia (YSZ) from CrysTec GmbH was heated to a set-point temperature. YSZ was used because it has a low thermal conductivity for a commercially available ceramic. The steady state temperature of the sample surface, here termed the background temperature ($T_{background}$), was measured via a K-type (chromel-alumel) TC. A K-type TC is used as it has a temperature range of −260 to 1370 °C, covering the minimum and maximum temperatures achievable in the ion beam end-station. The TC was previously calibrated by means of a ThermaSense infrared pyrometer. The background temperature was used as a reference point to determine the amount of beam heating and also to examine the background temperature dependence on the amount of beam heating.

The sample itself was mounted on a specialized high temperature sample holder manufactured by Thermionics Northwest Company. The holder comprises a stainless steel ring holding a 1 in. diameter Mo plate. Samples are mounted on the Mo plate through Mo clamps attached to the steel ring. A tungsten heating element is mounted behind the Mo plate. An external power supply can supply up to 9 A of current to the heating element. The resistance of the heating element is 0.9-1.1 Ω. Therefore, the maximum power supplied by the heating element is approximately 80 W. The sample manipulator at the center of the target vacuum chamber, to which the heating element and sample holder are mounted, is cooled via a cool N_2 vapor circuit behind the heating element and inside the sample manipulator. By adjusting the N_2 flux and external power supply, the temperature of the Mo plate can be increased or decreased. Ion irradiations carried out in this particular beam endstation can span a temperature range from −150 to 1200 °C. Sample temperatures can be maintained manually or via a feedback circuit and temperature controller. A Eurotherm PID controller allows for sample temperature measurements to be taken during irradiation. More details can be found in Ref. 13.

The Mo plate temperature is monitored with an auxiliary TC and a pyrometer mounted outside the vacuum chamber. Mo, having a high thermal conductivity (110-140 W m^{-1} K^{-1}) in the relevant temperature range, is a somewhat ideal material for mounting samples to in high temperature experiments. Inhomogeneities from the radiative heating distribution of the tungsten element on the backside of the Mo plate are smoothed out by efficient heat conduction within the plate. The uniformity of the temperature across the Mo plate has been verified by placing thermocouples at different locations on the plate and also by probing different areas of the plate with the pyrometer. It should be mentioned, however, that large thermal gradients can exist between the Mo plate and a sample. At cryogenic temperatures, no temperature gradient is observed even in low thermal conductivity samples (provided enough time for the sample and holder to reach thermal equilibrium). At high temperatures, however, significant radiative heat conduction from the sample surface prevents thermal equilibrium from occurring, thus a steady state temperature gradient appears. It is, therefore, of utmost importance to mount the thermocouple on the surface of the sample during high temperature irradiations. For small, irregularly shaped, or non-uniform samples, it is also important to mount the thermocouple as close to the irradiated area as possible.

The Au beam was rastered through 3×3 mm slits onto different areas of the sample. Four different configurations of thermocouple, Mo sample mounting clamp, beam area, and sample were used. These are shown in Fig. 1. In configurations (a) and (b), the ion beam is covering the TC junction. The junction is either nude (exposed to the ions) as in (b), or it is covered by an Mo clamp as in (a). The main purpose of comparing these configurations was to determine whether or not the clamp acts as a heat or charge sink. In configuration (c), the ion beam is placed over a portion of the YSZ sample away from the TC junction. This configuration (in comparison with (b)) helps determine if secondary electrons escaping from the TC wires or sample have a contribution to the measured beam heating. In configuration (d), there was no YSZ sample. Instead, the beam was placed on the TC junction with the junction in direct contact with the Mo plate of the sample holder. This configuration is used to tell if measurable beam heating is limited to poor thermal (and electronic) conductors or not.

In addition to steady state beam heating measurements, the heating and cooling transients were recorded with the TC controller when the beam was turned on and off, respectively.

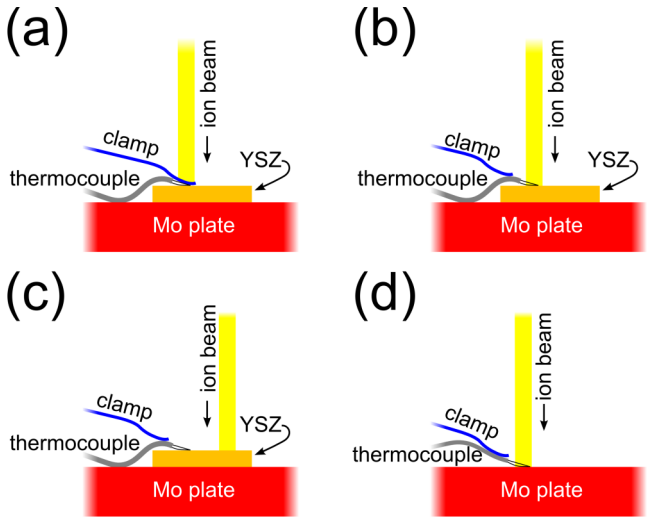

FIG. 1. Configurations of the ion beam heating experiments: (a) the irradiated area covers an Mo clamp in contact with the thermocouple (TC) junction, (b) the clamp rests on the ceramic insulators of the TC and the irradiated area covers the bare junction, (c) the TC junction is bare and the irradiated area covers a portion of the Yttria stabilized Zirconia (YSZ) sample ~2 mm away from the TC, (d) the irradiated area covers the bare junction which is directly in contact with the Mo plate of the sample holder.

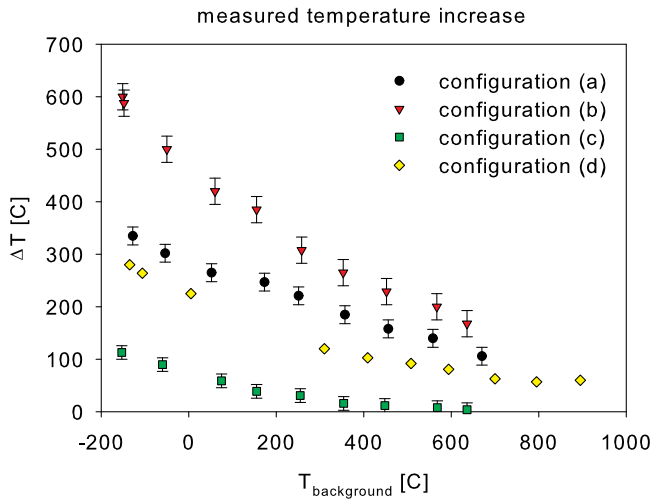

FIG. 2. Measured beam heating at different background temperatures for the YSZ sample with different thermocouple (TC) and beam geometries and for the Mo plate of the sample holder. The data key refers to the configurations from Fig. 1.

These transient data help determine the nature of the dominant conduction mechanisms responsible for the increase in temperature under irradiation. These were obtained with the beam area covering the thermocouple junction and with the Mo clamp attached to the ceramic elements of the thermocouple wire (configuration (b) of Fig. 1). The heating transients were recorded for 5 min.

III. RESULTS AND DISCUSSION

It was observed that the Mo plate of the sample holder can achieve much greater temperatures than at the surface of the YSZ sample. In other words, the sample never reaches thermal equilibrium due to radiative emission losses that begin to dominate at ~100 °C. Indeed, at low temperatures, where radiative emission does not take place to an appreciable extent, the YSZ and Mo surfaces were found to have identical temperatures. The inability of the sample to reach equilibrium is attributed to the low thermal conductivity of YSZ (1.8 W m^{-1} K^{-1} at 300 K).[14] From the perspective of designing high temperature experiments, it is important to measure the surface being irradiated since, in general, it is not possible to assume a sample is in thermal equilibrium with its holder/heater.

The steady state beam heating versus background temperature curves— shown in Fig. 2—reveal several interesting features. First, the beam heating can be large compared to the background temperature. A temperature increase of nearly 600 °C was observed at the lowest background temperature. Second, the amount of beam heating shows a strong dependence with background temperature. At lower temperatures, the beam heating is more extreme than at high temperatures. Third, away from the thermocouple, the beam can still perturb the measurement to a significant extent. Fourth, despite the insensitivity of the background temperature with the Mo clamp mounting position, the location of the Mo clip appears to significantly affect the amount of beam heating. The apparent contradiction here is predicated on the, perhaps, bad assumption that the TC's response to the filament heater and to the ion beam are both governed by heat transport processes alone. Finally, the beam heating effect is observed both in YSZ (a good thermal and electrical insulator) and also in Mo (a good thermal and electrical conductor). The large temperature increase and the effect of the Mo clamp position seem to suggest that the cause(s) of the measured beam heating is more electronic than thermal in nature. It is also important to note that, assuming the beam heating effect is an electronic effect, preparing insulating samples with thin conductive surface coatings will not necessarily completely mitigate the effect as it is also observed in Mo; a good electrical conductor. Such coatings, however, are known to reduce surface charging in insulators and so it is plausible that they could significantly reduce the artificial heating.[15] Additional experiments comparing the beam heating effect in different geometries in metal coated insulators, materials with low electronic conductivity and high thermal conductivity (e.g., diamond), and materials with high electronic conductivity and low thermal conductivity (e.g., thermoelectric materials) can help to more directly differentiate the contributions to the beam heating effect.

To further elucidate the cause of the heating, transient heating (beam on) and cooling (beam off) curves can be analyzed. These are shown in Figs. 3 and 4.

The time constants of the transient behavior are on the order of seconds; significantly greater than the integration time of the TC controller. The characteristic time constants are also background temperature dependent. Attempts to make single exponential fits to the transient data resulted in poor goodness-of-fit statistics. Fitting the data with double exponential curves, however, proved much more successful (all R values exceeded 0.999). The double exponential fits

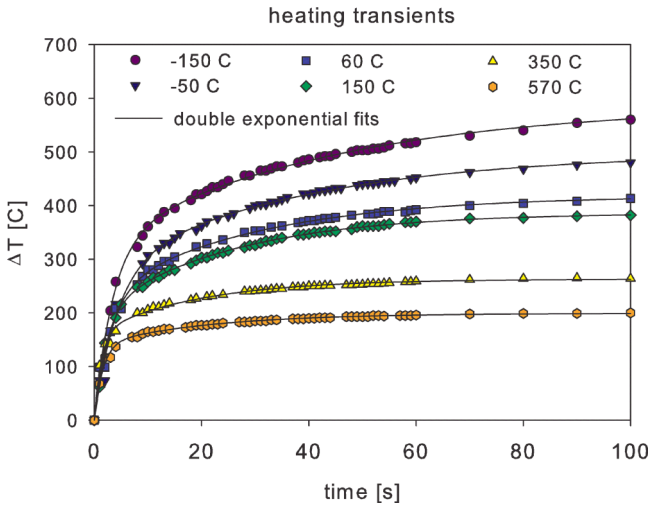

FIG. 3. Transient heating curves of YSZ at different background temperatures (indicated in the legend). The beam irradiation area is overlapping the thermocouple junction (configuration (b) in Fig. 1).

have the following form for the heating transients:

$$\Delta T = A_1\left[1-\exp\left(-\frac{t}{\tau_1}\right)\right]+A_2\left[1-\exp\left(-\frac{t}{\tau_2}\right)\right]. \quad (1)$$

A_1 and A_2 are pre-exponential factors and τ_1 and τ_2 are time constants. The equation for the cooling transients is

$$\Delta T = A_1\exp\left(-\frac{t}{\tau_1}\right)+A_2\exp\left(-\frac{t}{\tau_2}\right). \quad (2)$$

The behaviors of these coefficients as a function of background temperature are shown in Fig. 5. All coefficients decrease with increasing background temperature. In most cases, there is reasonable agreement between the coefficients during heating and cooling. This suggests that the transient behavior is not strongly coupled to ion effects (e.g., radiation induced conductivity). The possible exception is Fig. 5(d), which shows roughly a factor 2 enhancement of the τ_2 time constant at low temperature. This disagreement might be an indication that at low temperature, ion effects become

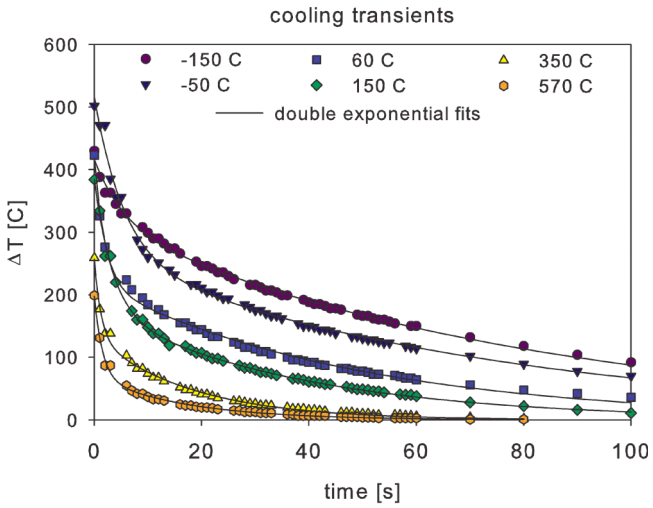

FIG. 4. Transient cooling curves of YSZ at different background temperatures (indicated in the legend). The beam irradiation area is overlapping the thermocouple junction (configuration (b) in Fig. 1).

significant in the charge (or heat) conduction mechanisms of the bulk sample. On the other hand, there may be unknown systematic errors in the data or the measurements themselves that are not fully accounted for in the fitting uncertainties.

In order to exclude the possibility that the measured beam heating is actually thermal in nature, numerical calculations of the beam heating were performed. For the given geometry of the sample, Mo plate, beam size, beam flux, and ion energy, the spatial temperature distribution at the surface of the YSZ sample was calculated by solving a discretized version of the heat equation. Figure 6 shows the two-dimensional distribution of the temperature increase on the sample surface for a 3×3 mm beam spot centered on a $5\times5\times0.5$ mm YSZ sample. Figure 7 shows the convergence of the maximum temperature change at the center of the beam. Each iteration represents a time step in the heat equation equal to $c_\rho\rho\times0.001$ K cm^3 W^{-1}, where c_ρ and ρ are the specific heat capacity and density of the material, respectively. Consequently, the time to achieve steady state is on the order of 0.1-1 s; significantly faster than the observed heating and cooling transients. The maximum temperature change reached is less than 25 °C under these conditions. That is far lower than the observed "heating."

It is worth noting that the background temperature is not considered in this calculation and only the change in temperature (the temperature increase) is calculated. This assumption relies on the linearity of the heat equation; heat sources are not coupled. In other words, the large heat source from the heating filament determines the background temperature in accordance with the heat equation but has no effect on the beam heating. The details of the filament heater contribution to the temperature are irrelevant as the only quantity of interest, the background temperature, can be measured directly. Meanwhile, the change in temperature is, to first order, independent of the background temperature and only dependent on the sample, geometry, and beam conditions (which are all well defined). In reality, there is a small coupling between the background temperature and beam-induced temperature change through the temperature dependent thermal conductivity. However, because the thermal conductivity of YSZ is roughly constant at the temperatures considered here,[16] and the beam-induced temperature perturbations are small, the assumption of linearity is reasonable. Essentially, the calculations support the hypothesis that the measured heating is not thermal in nature because the magnitudes of the changes are very different and the strong dependence on background temperature cannot be reproduced through the heat equation alone.

A validation of the model was performed by comparing its solution for a $10\times10\times10$ mm sample with an analytical solution for beam heating on a semi-infinite geometry in vacuum. Under these conductivity and beam conditions, a $10\times10\times10$ mm sample is a reasonable approximation of a semi-infinite medium. The analytical and discrete temperature maxima were found to be 82 °C and 85 °C, respectively. Truncation error and the finite size of the model can account for the remaining discrepancy.

The analytical solution begins from the stationary heat equation with a surface source term (actually a form of the

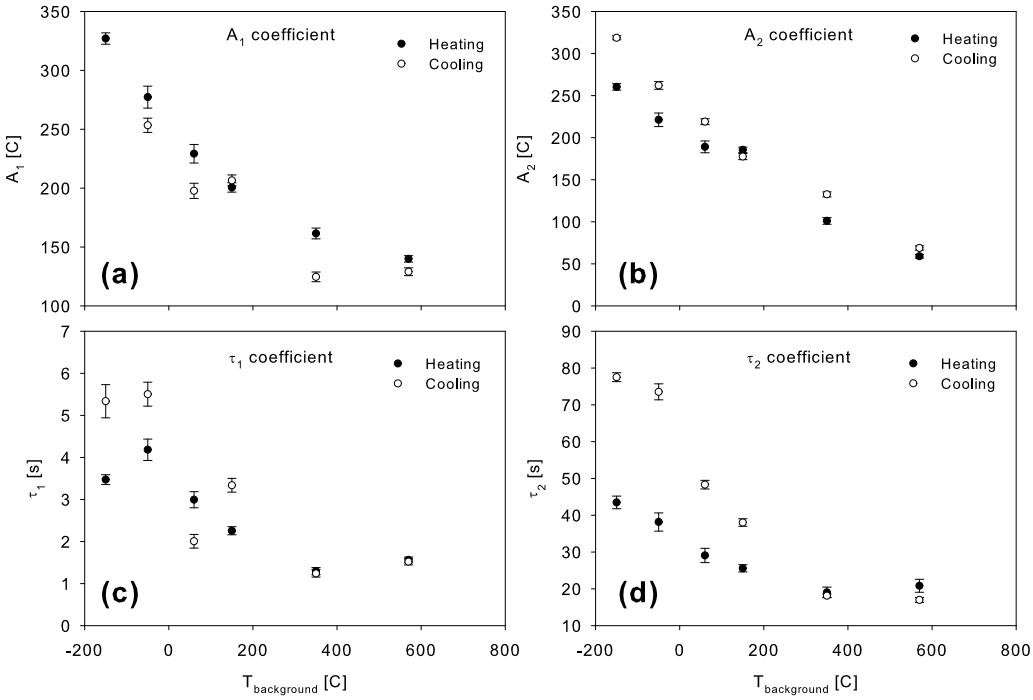

FIG. 5. Parameters of the two exponential fits to the heating and cooling transient curves. The pre-exponential factors A_1 and A_2 are shown in (a) and (b), respectively. The time constants τ_1 and τ_2 are shown in (c) and (d), respectively.

inhomogeneous Poisson equation) in a semi-infinite medium

$$k\nabla^2 u = q(x,y,z), \tag{3}$$

where k is the thermal conductivity, u is the temperature, and $q(x,y,z)$ is a spatially dependent heat rate given by

$$q(x,y,z) = \begin{cases} \phi E \delta(z) & \text{for } x,y \in (-l/2, l/2) \\ 0 & \text{otherwise} \end{cases}. \tag{4}$$

ϕ and E are the beam flux and energy. l is the side length of a square irradiation spot. For convenience, the areal heating rate can be written

$$\sigma = \phi E. \tag{5}$$

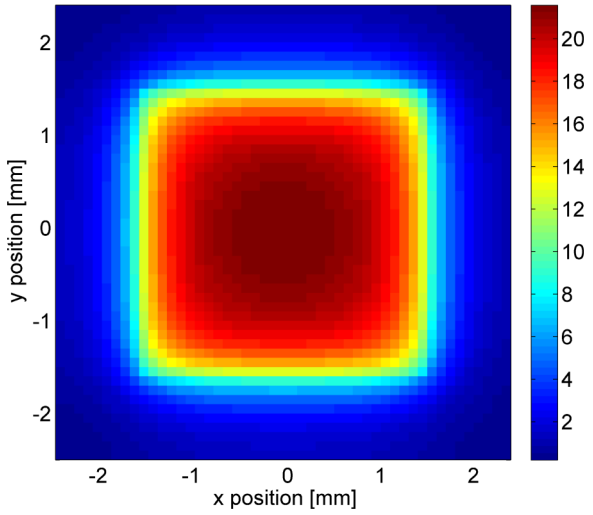

FIG. 6. Calculated steady state 2D spatial distribution of the temperature change of the 5×5×0.5 mm YSZ surface under 5.5×10^{12} cm^{-2} s^{-1} of 10 MeV Au^{3+} irradiation. The square beam spot has dimensions of 3×3 mm. The color scale bar represents the temperature increase in °C.

The only boundary condition is an adiabatic wall at the surface

$$\nabla u = 0 \text{ at } z = 0. \tag{6}$$

The solution involves directly integrating the Greens function solution for a delta function source, $\delta(x - x_0)\delta(y - y_0)\delta(z)$, over a square patch on the sample surface. The resulting temperature profile at the surface is given by

$$u(x,y,0) = \frac{\sigma}{2\pi k} f\left(-l/2 - y, l/2 - y, -l/2 - x, l/2 - x\right), \tag{7}$$

where

$$f(a,b,c,d) = g(b,d) + g(a,c) - g(a,d) - g(b,c), \tag{8}$$

$$g(d,b) = d\ln(\sqrt{d^2 + b^2} + b) + b\ln(\sqrt{d^2 + b^2} + d). \tag{9}$$

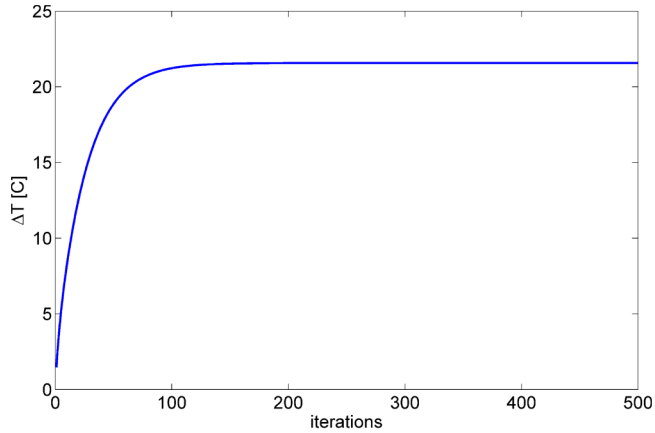

FIG. 7. Convergence of the sample temperature at the point of maximum beam heating.

The symmetric choice of the problem geometry gives a simple expression for the maximum temperature

$$u(0,0,0) = \frac{\sigma l}{\pi k} \ln\left(\frac{\sqrt{2}+1}{\sqrt{2}-1}\right) \approx 0.561 \frac{\sigma l}{k}. \quad (10)$$

The last result is interesting because it suggests a useful criterion for determining the maximum beam flux for an experiment with a square beam geometry,

$$\Delta T_{max} < 0.561 \frac{\sigma l}{k}. \quad (11)$$

Because the analytical solution is semi-infinite, does not account for radiative losses or other heat losses, and assumes that all ion energy is deposited as heat (not valid for insulators where ion beam induced luminescence also occurs[4,17]), then as long as the thermal conductivity of the sample is less than the thermal conductivity of the sample holder, the above expression represents a conservative estimate of the temperature increase. Therefore, it can be used to estimate the upper limit of the beam heating for a given experiment. Indeed, the 82 °C value calculated assuming the experimental beam conditions in the infinite slab geometry is greater than the 21 °C value determined from the discretized heat equation calculations for the more realistic sample size and geometry.

The heat equation calculations show that the real beam heating cannot account for the measured heating (or at least the majority of it). An alternative explanation for the phenomena must be provided. One possible explanation relies on the creation of secondary electrons on the TC wires. A thermocouple exploits a differential thermoelectric effect in two dissimilar alloys. A TC junction comprises a weld between two such alloys. Irradiating each wire will produce secondary electrons that can escape the metal and remove negative charge. In general, the work functions for each alloy are different and thus the efficiencies for producing secondary electrons are different (for the same ion energy and flux). Therefore, the net current away from each wire differs and a compensating electromotive force (EMF) will form. Such an EMF can result in an erroneous measurement in the TC controller. In light of the results in Fig. 2, showing the same beam heating effect when the beam area is separated from the TC junction by 2 mm, this effect is probably weak if not negligible since no secondary electrons are produced in the TC wires in that situation. An alternative explanation relies on an electrostatic potential created around the irradiated area.

Depositing charge on an insulator, such as YSZ, mounted on a conductive plate is akin to charging a capacitor. A large temperature difference was measured between the Mo plate of the sample holder and the surface of the YSZ. Evidently, a large thermal gradient forms across the sample. Insulators are known to have temperature dependent electrical conductivities. The thermal gradient could result in a spatially dependent conductivity, hence a depth-dependent leakage resistance in the capacitor. Imagining that the equipotential surfaces inside the material divide it into a number of layers, each characterized by a capacitor and temperature sensitive resistor in parallel, reassembling the layers is equivalent to connecting them in series. The simplest model—a uniform temperature model—replaces the many layers by one layer with a single capacitor and resistor in parallel. In this model, the ion beam is replaced with a current source connected in series to the sample circuit. This model yields exponential growth and decay of the heating/cooling transient when the ion beam is turned on and off, respectively. The actual transient data, however, are better modeled with double exponential behavior. To modify the model, two capacitor-resistor layers are used instead (see Fig. 8). In other words, the temperature gradient is divided into two temperature regions; a high temperature, T_2, and low temperature, T_1, region.

With this modification, the double exponential behavior is reproduced. The voltage measured at the thermocouple is given by

$$\Delta V \approx i\left\{R_1\left[1-\exp\left(-\frac{t}{R_1C_1}\right)\right] + R_2\left[1-\exp\left(-\frac{t}{R_2C_2}\right)\right]\right\}, \quad (12)$$

i is the ion beam current. In fact, it would be more physically accurate to consider the sample as an arbitrary number of multiple layers. This gives a multi-exponential behavior. According to the fit statistics, however, two layers are already sufficient for describing the transient behavior. The actual temperature measurement is related to the effect of the additional voltage on the thermocouple. With the ion beam off, biasing the thermocouple through the sample holder grounding cable with a 300 V battery was found to increase the temperature reading by ~40 °C in one polarity and decrease the reading by the same amount when biased with the opposite polarity. The actual dependence between the localized potential on the sample surface and the measurement of the temperature is likely complicated as it depends not only on the shape and magnitude of the potential but also on the calibration of the thermocouple. Nevertheless,

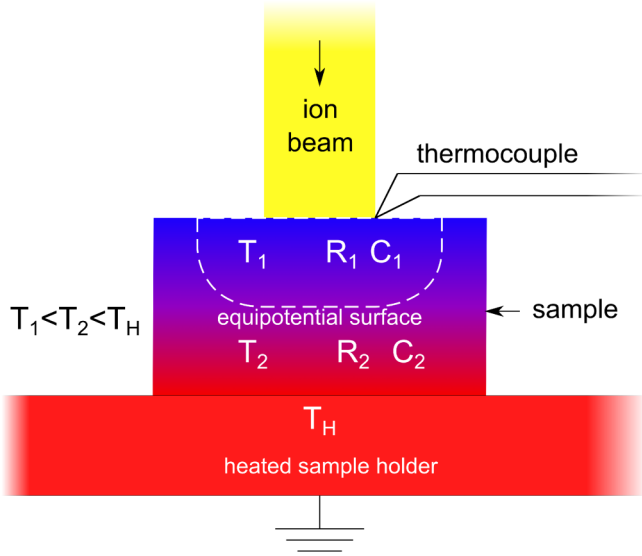

FIG. 8. Model explaining the artificial heating effect under ion beam irradiation. Positive charge from the ion beam builds up on the surface and discharges through the bulk and along the surface of the sample, thereby creating a localized electrical potential. Due to thermal gradients, the sample acts like a series of simple circuits (each with a capacitor and resistor in parallel). A two circuit model is sufficient to account for most of the transient behavior of the measured heating.

the effect of an external potential at the TC junction appears to modify the measured temperature.

According to this model and Fig. 5, the resistivity of the sample decreases as background temperature increases. This is consistent with the theory of electrical conduction in semiconductors and insulators where the creation of charge carriers requires thermal excitation above an activation energy. In other words, the carrier mobility is usually expected to be temperature dependent. At low temperatures, the charge carriers are fairly immobile, hence a potential can buildup near the irradiated area. Furthermore, the low carrier mobility results in a slow discharge process (i.e., comparatively large time constants). Conversely, at high temperatures, the carriers are relatively mobile, hence less potential builds up in the steady state condition and the charging and discharging processes are more rapid (smaller time constants). That said, conduction processes involved in the measurements presented in this manuscript are likely more complex as irradiation induced conductivity, surface conduction, and discharge through the TC could also contribute. Additional experiments with different materials, ion species, and energies could be useful in corroborating this model. This simple model is capable of correctly describing the observed phenomenology of the beam heating effect without making any assumptions of exotic physical mechanisms.

IV. CONCLUSIONS

The ion beam heating effect was investigated over a temperature range of −170 to 900 °C with a 10 MeV Au^{3+} ion beam in YSZ. The main results indicate that thermocouple measurements show an extreme temperature increase at low temperatures and become less dramatic at high temperature. Comparison with numerical heat equation calculations indicates that the measured increase cannot be fully ascribed to true beam heating (as described through a heat deposition and transport process). Electronic effects likely play a role. A simple model was invoked to describe the observed behavior. It relies on the assumption that the ion beam induces an electrostatic potential in the ceramic material perturbing the thermocouple's sensing ability. Knowing that the ion beam heating effect can, in some circumstances, be largely artificial is important in conducting an accurate temperature measurement with a thermocouple. Indeed, using a thermostated ion irradiation facility with a thermocouple in a feedback loop with a heating controller (or a cooling-heating system) is a seemingly attractive experimental setup, especially for long irradiations/analyses where stable temperature control is desired. Such a setup, however, would be susceptible to the artificial beam heating effect as a spurious temperature increase would cause the feedback system to drive the true temperature down to match the temperature set point. In a reversed polarity setup, the temperature would rise, perhaps even damaging the sample or the system. Consideration of the artificial beam heating effect should be made in designing high dose rate experiments/analyses.

ACKNOWLEDGMENTS

This work was primarily supported by the U.S. Department of Energy (DOE) Nuclear Energy University Programs. M. L. Crespillo and J. T. Graham are grateful to support from the University of Tennessee Governors Chair program.

[1]J. F. Fowler, Phys. Med. Biol. **3**, 395 (1959).
[2]E. R. Hodgson and T. Shikama, in *Comprehensive Nuclear Materials Vol. 4*, edited by R. J. M. Konings, T. R. Allen, R. E. Stoller, and S. Yamanaka (Elsevier, Amsterdam, The Netherlands, 2012), pp. 701–724.
[3]S. M. Gonzalez, A. Moroño, D. E. Hole, and E. R. Hodgson, J. Nucl. Mater. **386-388**, 1006 (2009).
[4]P. D. Townsend, M. Khanlary, and D. E. Hole, Surf. Coat. Technol. **201**, 8160 (2007).
[5]P. D. Townsend and Y. Wang, Energy Procedia **41**, 64 (2013).
[6]R. J. Brooks, D. E. Hole, and P. D. Townsend, Nucl. Instrum. Methods Phys. Res., Sect. B **190**, 136 (2002).
[7]P. J. Schultz, C. Jagadish, M. C. Ridgway, R. G. Elliman, and J. S. Williams, Phys. Rev. B **44**, 9118 (1991).
[8]G. Dearnaley, J. H. Freeman, R. S. Nelson, and J. Stephen, *Ion Implantation* (North-Holland, New York, 1973).
[9]P. D. Parry, J. Vac. Sci. Technol. **13**, 622 (1976).
[10]M. J. Kim and R. W. Carpenter, Ultramicroscopy **21**, 327 (1987).
[11]T. Ishitani and H. Kaga, J. Electron Microsc. **44**, 331 (1995).
[12]J. Kempf, M. Nonnenmacher, and H. H. Wagner, Appl. Phys. A **56**, 385 (1993).
[13]Y. Zhang, M. L. Crespillo, H. Xue, K. Jin, C. H. Chen, C. L. Fontana, J. T. Graham, and W. J. Weber, Nucl. Instrum. Methods Phys. Res., Sect. B **338**, 19 (2014).
[14]K. W. Schlichting, N. P. Padture, and P. G. Klemens, J. Mater. Sci. **36**, 3003 (2001).
[15]J. Kim, W. Hong, H. J. Woo, and C. H. Eum, J. Korean Phys. Soc. **43**, 582 (2003).
[16]N. Wang, H. Chen, H. He, W. Norimatsu, M. Kusunoki, and K. Koumoto, Sci. Rep. **3**, 3449 (2013).
[17]P. D. Townsend and M. L. Crespillo, Phys. Procedia **66**, 345 (2015).